

Article

Macrophages Promote Tumor Cell Extravasation across an Endothelial Barrier through Thin Membranous Connections

Alessandro Genna ^{1,†} , Camille L. Duran ^{2,3,4,†} , David Entenberg ^{3,4,5,6,7} , John S. Condeelis ^{2,4,5,6,7} and Dianne Cox ^{1,4,6,7,*} 

¹ Department of Developmental and Molecular Biology, Albert Einstein College of Medicine/Montefiore Medical Center, Bronx, NY 10461, USA

² Department of Cell Biology, Albert Einstein College of Medicine/Montefiore Medical Center, Bronx, NY 10461, USA

³ Department of Pathology, Albert Einstein College of Medicine/Montefiore Medical Center, Bronx, NY 10461, USA

⁴ Gruss-Lipper Biophotonics Center, Albert Einstein College of Medicine/Montefiore Medical Center, Bronx, NY 10461, USA

⁵ Integrated Imaging Program, Albert Einstein College of Medicine/Montefiore Medical Center, Bronx, NY 10461, USA

⁶ Cancer Dormancy and Tumor Microenvironment Institute, Albert Einstein College of Medicine, Bronx, NY 10461, USA

⁷ Montefiore Einstein Cancer Center, Albert Einstein College of Medicine, Bronx, NY 10461, USA

* Correspondence: dianne.cox@einsteinmed.edu

† These authors contributed equally to this work.

Simple Summary: Breast cancer is one of the most common cancers in women and despite improvements in treatments, patients suffering from metastatic disease still have a very low survival rate. A rate-limiting step is the seeding of tumor cells from the blood into the metastatic site. Macrophages are a key cell type in the metastatic niche, which are important for tumor cell seeding despite being separated from the tumor cells in the vasculature by an endothelial barrier. We found that macrophages and tumor cells make thin membranous connections through the endothelial barrier to assist in tumor cell crossing. These structures are similar to tunneling nanotubes that we previously showed were important for tumor cell invasion. We found that these macrophage-mediated connections were important for tumor crossing the endothelial barrier and for metastatic seeding. This new finding suggests that targeting tunneling nanotubes may limit tumor spread.

Abstract: Macrophages are important players involved in the progression of breast cancer, including in seeding the metastatic niche. However, the mechanism by which macrophages in the lung parenchyma interact with tumor cells in the vasculature to promote tumor cell extravasation at metastatic sites is not clear. To mimic macrophage-driven tumor cell extravasation, we used an in vitro assay (eTEM) in which an endothelial monolayer and a matrigel-coated filter separated tumor cells and macrophages from each other. The presence of macrophages promoted tumor cell extravasation, while macrophage conditioned media was insufficient to stimulate tumor cell extravasation in vitro. This finding is consistent with a requirement for direct contact between macrophages and tumor cells. We observed the presence of Thin Membranous Connections (TMCs) resembling similar structures formed between macrophages and tumor cells called tunneling nanotubes, which we previously demonstrated to be important in tumor cell invasion in vitro and in vivo. To determine if TMCs are important for tumor cell extravasation, we used macrophages with reduced levels of endogenous M-Sec (TNFAIP2), which causes a defect in tunneling nanotube formation. As predicted, these macrophages showed reduced macrophage-tumor cell TMCs. In both, human and murine breast cancer cell lines, there was also a concomitant reduction in tumor cell extravasation in vitro when co-cultured with M-Sec deficient macrophages compared to control macrophages. We also detected TMCs formed between macrophages and tumor cells through the endothelial layer in the eTEM assay. Furthermore, tumor cells were more frequently found in pores under the endothelium that contain macrophage protrusions. To determine the role of macrophage-tumor cell TMCs in vivo, we



Citation: Genna, A.; Duran, C.L.; Entenberg, D.; Condeelis, J.S.; Cox, D. Macrophages Promote Tumor Cell Extravasation across an Endothelial Barrier through Thin Membranous Connections. *Cancers* **2023**, *15*, 2092. <https://doi.org/10.3390/cancers15072092>

Academic Editor: Emil Lou

Received: 16 February 2023

Revised: 23 March 2023

Accepted: 29 March 2023

Published: 31 March 2023



Copyright: © 2023 by the authors. Licensee MDPI, Basel, Switzerland. This article is an open access article distributed under the terms and conditions of the Creative Commons Attribution (CC BY) license (<https://creativecommons.org/licenses/by/4.0/>).

generated an M-Sec deficient mouse. Using an in vivo model of experimental metastasis, we detected a significant reduction in the number of metastatic lesions in M-Sec deficient mice compared to wild type mice. There was no difference in the size of the metastases, consistent with a defect specific to tumor cell extravasation and not metastatic outgrowth. Additionally, with an examination of time-lapse intravital-imaging (IVI) data sets of breast cancer cell extravasation in the lungs, we could detect the presence of TMCs between extravascular macrophages and vascular tumor cells. Overall, our data indicate that macrophage TMCs play an important role in promoting the extravasation of circulating tumor cells in the lungs.

Keywords: breast cancer; metastasis; macrophages; thin membranous connections; tunneling nanotubes; extravasation; M-Sec

1. Introduction

During the past several decades, much effort and focus has been put into fighting primary breast cancer growth, which has led to an increase in survival rate (90% five-year relative survival) for patients with non-disseminated tumors. In contrast, patients suffering from metastatic disease have a very low (28% five-year) relative survival rate [1]. The poor outcome in cases of metastatic disease has led to an intense study of the metastatic process. Metastasis results from a sequence of events that starts in the primary tumor and allows tumor cells to intravasate into the blood stream and use the circulatory system to reach distant organs [2–4]. Viable circulating tumor cells (CTCs) that extravasate into the parenchyma of distant organs can then either colonize the organ (leading to overt metastases) or survive in a dormant state while still retaining the ability to produce metastases at a later time, depending on the microenvironment [5,6].

Macrophages are an important player involved in the metastatic process. Macrophages are very diverse and contain many subpopulations that fulfill different functions including tissue repair, mediation of inflammatory responses, and promotion of tumor progression. Many studies show a strong correlation between high infiltrating macrophage levels in the primary tumor and increased metastatic burden [7,8]. Macrophages aid tumor cells in the primary tumor by promoting tumor cell growth, migration, and invasion, and are referred as tumor associated macrophages (TAMs). TAMs have been shown to secrete EGF and co-migrate in streams with tumor cells towards blood vessels [9–11]. In the perivascular region, a subpopulation of Tie2^{high} expressing macrophages, along with stationary tumor cells in a structure identified as a TMEM doorway, play an important role in the intravasation of tumor cells. These macrophages mediate intravasation by creating a local transient opening in the blood vessel [12]. Perivascular macrophages are also responsible for inducing tumor stemness and dormancy that prepares the tumor cells to colonize and survive at distant organs [5,13]. Other data indicating the importance of macrophages in metastases are the requirement of colony-stimulating factor 1 (CSF-1) for metastatic dissemination, an essential factor for macrophage survival and proliferation [14,15]. Furthermore, a unique population of macrophages called Metastases Associated Macrophages (MAMs), characterized by the surface markers F4/80+/CSF-1R+/CD11b+/Gr1-CX3CR1^{high}/CCR2^{high}/VEGFR1^{high}, are recruited to the lungs and are important for the number and size of metastases in the PyMT experimental metastasis model [16,17]. Furthermore, MAMs are required for efficient metastatic seeding and present a specific expression pattern that promotes their accumulation and metastatic seeding [18,19].

It was previously noted in time-lapse intravital images that tumor cell-macrophage interactions dramatically increased during tumor cell extravasation [20]. This interaction occurred despite the fact that 70% of the tumor cells were still located in the vasculature. Additionally, when tumor cells were captured in the act of extravasation (crossing the vessel), macrophages appeared to directly interact with the extravasated part of the tumor

cell [21,22]. Additionally, when in association with tumor cells, macrophages extended extremely long, thin pseudopods that would not be visible at a lower resolution [21].

The existence of membranous connections between cells *in vivo* was first demonstrated by Chinnery in 2008, describing membranous nanotubes between immune cells and stromal cells in the mouse cornea [23]. Similar structures can be found connecting perivascular macrophages to resident tissue cells and between pericytes on separate capillary systems [24,25]. Membranous connections have been described in various tumor types [26]. In glioblastoma, they play a role in chemoresistance, and similar structures have been found by light sheet microscopy to be present in MDA-MB-231 brain metastases [27,28]. These structures are often called different names such as membrane nanotubes [23], tumor microtubes [27], or tunneling nanotubes (TNTs) [29,30] and can be distinguished by diameter, cytoskeletal components, and whether they are closed-ended or open-ended. However, they all fall under the broad category of thin membranous connections (TMCs). These structures have been proven to have the ability to promote different functions such as exchanging mitochondrial and nuclear material, potentiating growth factor signaling, and promoting ion exchange [28,31–33]. All these different functions are mediated by establishing direct cell-to-cell contact and communication between distant cells [34]. M-Sec (TNFAIP2) is an important regulator of TNT-like membranous connections in macrophages, tumor cells, and other cell types [35]. M-Sec is a 73 KDa cytosolic protein whose N-Terminal polybasic region is responsible for M-Sec recruitment to the plasma membrane and its C-terminus recruits RalA, thereby regulating the exocyst function needed for TMC formation [36,37]. Our previous work has shown that macrophage TNTs enhance tumor cell invasion *in vitro* and in a zebrafish model of invasion [33].

Despite the importance of macrophages in tumor cell extravasation, the events leading to extravasation have not been completely elucidated. Here, our results using an *in vitro* assay, which mimics extravasation, demonstrate that macrophage TMCs play a major role in promoting tumor cell extravasation. We used an M-Sec deficient mouse, whose macrophages have a defect in TMC formation, to confirm the importance of macrophage TMCs *in vivo*. Furthermore, using high-resolution intravital-imaging (IVI) to examine the interaction of macrophages with tumor cells during extravasation, we observed a macrophage in the lung parenchyma interacting with a tumor cell via a TMC prior to extravasation.

2. Materials and Methods

2.1. Cell Lines and Culture Media

MDA-MB-231 cells were purchased from ATCC and cultured in DMEM supplemented with 10% FBS and penicillin-streptomycin antibiotics. Before the start of experiments, MDA-MB-231 cells were serum-starved for 16 h in DMEM supplemented with 0.5% FBS/0.8% BSA. Human umbilical vein endothelial cells (HUVECs, Lonza, Allendale, NJ, USA) were used between passages 1–4 and were cultured in EGM-2 (Lonza, Allendale, NJ, USA). All cells were cultured and maintained in a 5% CO₂ and 37 °C incubator. Murine monocyte/macrophage RAW264.7 subline LR5 [38] was cultured in RPMI 1640 medium (Mediatech/Corning, Corning, NY, USA) supplemented with 10% heat-inactivated newborn calf serum (Sigma-Aldrich, Burlington, MA, USA) and antibiotics. Bone marrow-derived macrophages (BMMs) were isolated from the tibia and femurs of genotyped female mice as described [39] and grown in α MEM with 15% heat-inactivate FBS, 36 ng/mL recombinant human CSF-1 (kindly provided by ER Stanley), and antibiotics. E0771 medullary breast adenocarcinoma cells were originally isolated from a spontaneous breast tumor in C57BL/6 mice. The E0771-GFP cells were kindly provided by Dr. Lalage Wakefield (NIH-NCI), who obtained them from Dr. Fengzhi Li in Dr. Enrico Mihich's lab (Roswell Park Cancer Institute, Buffalo, NY, USA).

2.2. Antibodies and Reagents

Most reagents including Cell-Tracker Red (CMPTX) cat #C34552 and Cell-Tracker Green (CMFDA) cat #C7025 were obtained from Thermo Fisher. ZO-1 Polyclonal Antibody (Invitrogen, Waltham, MA, USA, cat #40–2200) and M-Sec/TNFAIP2 (Abcam, Cambridge, UK, ab91235) antibodies were used for immunofluorescence and anti-actin (Sigma, Burlington, MA, USA) or anti-TNFAIP2 (Invitrogen, Waltham, MA, USA, PA5-13542) were used in western blotting.

2.3. Mice

All procedures were conducted in accordance with the National Institutes of Health regulation concerning the care and use of experimental animals and with the approval of the Albert Einstein College of Medicine Animal Care and Use Committee (protocol 00001274). The TNFAIP2 KO mouse model was generated by CRISPR technology. In brief, a guide RNA (gRNA) targeting exon2 of TNFAIP2 gene, Tnfaip2 Ex2 gRNA 62/85 (targeting sequence: aaagccagctctacatccgagg) was designed by online software Benchling (www.benchling.com, accessed on 6 March 2019, San Francisco, CA, USA) and generated by in vitro transcription. Cas9 protein was purchased from PNB. All the above CRISPR ingredients were injected into the fertilized eggs of C57BL6 mice and then the injected fertilized eggs were transferred to the pseudopregnant CD1 female mice for the production of offspring. TNFAIP2 genotyping was carried out using primers F: AGCTGTGCATTTAGGTCCAT and RW: TGTGGGCAGTGGACCATCTA. Loss of M-Sec protein was confirmed by western blotting using an M-Sec specific antibody. Homozygous M-Sec-KO mice were viable, born at normal Mendelian ratios, grew normally, and showed a normal phenotype similar to that reported using a M-Sec deficient mouse generated by the Riken Centre [40]. For the intravital imaging MacBlue C57BL6 mice, Tg(Csf1r*-GAL4/VP16,UAS-ECFP)1Hume/J (Stock No: 026051, Jackson Laboratory) expressing ECFP under the control of a truncated CSF-1r promoter were crossed with B6.Cg-Gt(ROSA)26Sortm14(CAG-tdTomato) to label the vasculature with tdTomato utilizing Cre driven by Cadh5 endothelial promoter, as described in [22]. All ECFP⁺ cells in peripheral blood of MacBlue mice are CD11b-positive, negative for lymphocyte markers, and all ECFP^{hi} leukocytes express the monocyte/macrophage marker F4/80.

2.4. Western Blot

Whole-cell lysates for western blotting were created by lysing cells in ice-cold buffer containing 1% Triton X-100, 25 mM Tris-HCl, 137 mM NaCl, and a protease inhibitor cocktail (2 mM EDTA, 1 mM benzamidine, 1 mM orthovanadate, 10 µg/mL aprotinin, and 10 µg/mL leupeptin). Lysates were resolved using SDS-PAGE, and proteins were then transferred onto PVDF membranes (Immobilon-P, EMD Millipore, Burlington, MA, USA). Membranes were subsequently blocked (10% non-fat milk in TBS with 0.1% Tween-20 (TBST)) before incubation with primary antibodies at 4 °C overnight. Membranes were washed with TBST and then incubated with HRP-conjugated secondary antibodies. Images were acquired and analyzed using a Kodak Image Station 440.

2.5. Extravasation Trans-Endothelial Migration (eTEM) Assay

Transwell inserts containing 8 µm sized pores (Millipore, Burlington, MA, USA) were coated with 50 µL of growth factor reduced matrigel (BD BioSciences, San Jose, CA, USA), diluted in DMEM media (Invitrogen, Waltham, MA, USA) to 300 µg/mL, for 1 h at 37 °C. Then, 1×10^5 HUVECs were seeded onto the matrigel-coated filters in 300 µL EGM-2 in the upper chamber of the transwell and equilibrated with 650 µL of EGM-2 in the well. Transwells were incubated in a 24 well plate containing complete media at 5%CO₂/37 °C for 48 h. To check the integrity of the endothelium, we used a vascular permeability assay to determine the lack of leakage of high molecular weight dextran from one side of the HUVEC monolayer through the transwell into the lower well. Next, 6×10^4 cell tracker-red labeled macrophages were added to the underside of the transwell containing

an endothelial monolayer and allowed to adhere for 2 h at 5%CO₂/37 °C while positioned upside down in a clean 20 cm plate. Transwells were then returned to the 24 well plate and 2×10^4 serum starved cell tracker green-labeled tumor cells were added into the upper side of the chamber and incubated at 5%CO₂/37 °C. To determine the amount of tumor cell trans-endothelial migration, after 18 h, transwells were washed with PBS two times and then fixed with 4% paraformaldehyde/PBS for 20 min. Cells were then permeabilized for 10 min using 0.1% Triton X-100 in PBS and then stained with antibodies against ZO-1 (Invitrogen, Waltham, MA, USA) to label the endothelium. To image the eTEM assay, transwells were placed on a MatTek dish (MatTek Corporation, Ashland, MA, USA) in PBS and then imaged on a previously described custom-built inverted multiphoton microscope with a Spectra Physics Mai Tai-DeepSee laser set to 880 nm and a 25X, NA 1.05, water immersion objective [41]. Then, 1 µm step Z-stacks were acquired, which spanned the depth of the transwell. Post assay, we verified the presence of tight junctions between the endothelial cells using the ZO-1 staining. Only areas of the filter where the endothelial layer was intact with no gaps between the endothelial cells were used for analyses. During quantification of tumor cell trans-endothelial migration, only the tumor cells (cell tracker-green labeled) that had breached the endothelium (ZO-1 stained) were scored as trans-endothelial migration events.

2.6. TMP Quantitation and Proximity Analysis

The ability of either macrophages or tumor cells to make a thin membranous protrusion (TMP) across the filter and the endothelium was determined and quantified. In brief, the eTEM assay was assembled as described above and fixed at 1 h, 2 h, and 3 h after tumor cell seeding. The transwells were then permeabilized, stained as described above, and Z-stack images of the filter were taken. In order to be scored as a TMP in the eTEM assay, a cell protrusion must be at least 8 µm in length and has to cross the filter in the Z-Stack series while the main cell body remains on the originally seeded face of the chamber. Data were reported as the average number of TMPs present per field in a minimum of 25 fields per condition. To determine the probability of finding tumor cells in proximity of macrophages, a circle with a radius of 30 µm was drawn around a pore with macrophages on the extra-vasculature space in the images of the underside of the filter using ImageJ, which was defined as a region of interest (ROI). The ROI was then imported onto the corresponding image of the vascular side of the transwell and the presence of tumor cells within the circle was scored as a positive event. Data were then reported as the percentage of the time that tumor cells are found in proximity (within 30 µm radius) to macrophages either with or without protrusions into the filter.

2.7. TMC Quantitation

The ability of cells to make TMCs in vitro was monitored following culture of RAW/LR5 or BMMs overnight in 35 mm MatTek dishes (MatTek Corporation, Ashland, MA, USA) in complete growth medium. Cells were briefly washed with PBS buffer and then imaged live so as to avoid the TMC breakage that occurs during fixation. In order to be counted as a TMC connection, at least one TMC of at least 8 µm in length was required to be present between two cells with at least a portion of the TMC not adherent to the substratum. To be categorized as TMC negative, cells without TMCs were required to be within one cell body length of another cell without touching any other cell. TMCs were also quantified in the eTEM assay. The eTEM assay was performed as described above (see in vitro extravasation assay) and fixed after 1, 2, or 3 h.

2.8. Quantification of Lung Metastasis

E0771-GFP tumor cells were trypsinized and passed through a 40 µm cell strainer (Corning, Corning, NY, USA, cat #352340) in order to remove tumor cell clumps. Then, 2×10^5 cells were resuspended in 100 µL sterile PBS and intravenously (*iv*) injected into the lateral tail vein. Lungs were harvested 1 week after injection and GFP positive tumor

cells were counted via epifluorescence microscopy using a 20X phase objective mounted on an Olympus IX71 microscope. Quantification of lung metastases was scored by counting metastatic foci which contained >5 cells. Images of metastatic nodules were taken with a Sensicam cooled CCD camera. Images were thresholded in ImageJ (National Institutes of Health) and the size of nodules was quantified using the analyze particles function.

2.9. Window for High Resolution Imaging of the Lung (WHRIL) and Intravital Imaging

The window for high resolution imaging of the lung (WHRIL) implantation surgery was performed as described previously [22,42]. Briefly, mice were anesthetized and the soft tissue was removed from the upper left chest. The 6th and 7th rib were partially removed, exposing the lung tissue. A lung window frame was inserted between the gap in the chest wall and sutured in place. The underside of the lung window was adhered to lung tissue by applying positive end-expiratory pressure. A 5 mm coverslip was glued to window frame and attached to the exposed lung tissue. The ribs were cinched within the window frame groove using a purse-string suture. The skin was cinched into the same window frame groove using another purse-string suture. Excess air was removed by inserting an insulin syringe into the thoracic cavity through the diaphragm. For imaging, one day after window implantation, anesthesia was induced using 5% isoflurane, windows were secured within a fixturing plate and animals were placed on the microscope stage. E0771-GFP cells were injected via the tail vein (as described above). A heated chamber was placed around the animal during the course of imaging and maintained at physiological temperatures by a forced-air heater (AirTherm ATX, WPI Inc., Sarasota, FL, USA). The animals were maintained at 0.75–1.5% isoflurane for the duration of imaging. Imaging on a custom-built, inverted multiphoton microscope equipped with a 25X NA 1.05 water immersion objective and a Spectra Physics Mai Tai-DeepSee laser set to 880 nm [41] was performed as previously described. Z-stacks (21 μ m deep, 3 μ m step size) time lapse imaging (one stack every 1.4 min for 8 h) was acquired using two frame averages in 16 bit using a 25 \times 1.05 NA objective lens.

3. Results

3.1. Macrophage TMCs Are Important in Promoting Tumor Cell Extravasation In Vitro

Macrophages play an important role in promoting metastatic seeding [18,19] and we previously detected stromal macrophages in contact with tumor cells arriving at the metastatic site [22]. However, it is unclear how macrophages in the lung parenchyma interact with CTCs in the vasculature. To specifically study the role of TMCs connecting macrophages to tumor cells through an endothelium, we employed an in vitro assay that mimics macrophage-assisted tumor cell extravasation, maintaining the physical characteristics, the physiology, and cellular orientation of macrophages and tumor cells in the lung vasculature (Figure 1A) [16]. We cultured a highly metastatic triple negative breast cancer cell line (MDA-MB-231) on a transwell membrane coated with an intact layer of endothelial cells. The endothelial layer separated the tumor cells from cells of a murine derived macrophage cell line (RAW 264.7/LR5) that were attached to the bottom of the filter. We could detect a small but insignificant amount of tumor cell crossing into the extravascular space (bottom of the chamber) starting an hour after the addition of tumor cells (Figure 1B). During this period, we observed macrophage membrane extensions spanning the endothelial layer and the filter's pores connecting to tumor cells (TMCs). TMCs could be detected two hours post tumor cell seeding (Figure 1C,D). We then determined the frequency of tumor cells or macrophages to make thin membranous protrusions (TMPs) or connections (TMCs) into the layer between the two cell types over time. While not significant, macrophages seem to generate a greater number of protrusions compared to tumor cells (Figure 2A). We also investigated the conditions under which these macrophage protrusions occur in response to tumor cells. We determined whether there was an association between macrophages forming protrusions and the presence of tumor cells on the upper side of the endothelium in the vascular space. We measured the association of

macrophages with or without protrusions through a pore towards the endothelial layer with the presence of tumor cells on the vascular side of endothelium within a diameter of 60 μm centered on the pore (Figure 2B). Our data shows that tumor cells are found more frequently associated to areas with macrophages containing protrusions (86%), while there was only a random association between macrophages without protrusions and tumor cells (48%) (Figure 2C,D). These data indicate that tumor cells are preferentially localized to areas above macrophages containing protrusions. However, it is unclear whether macrophage protrusions are being directed towards tumor cells, or whether tumor cells migrate towards sites above macrophages with protrusions.

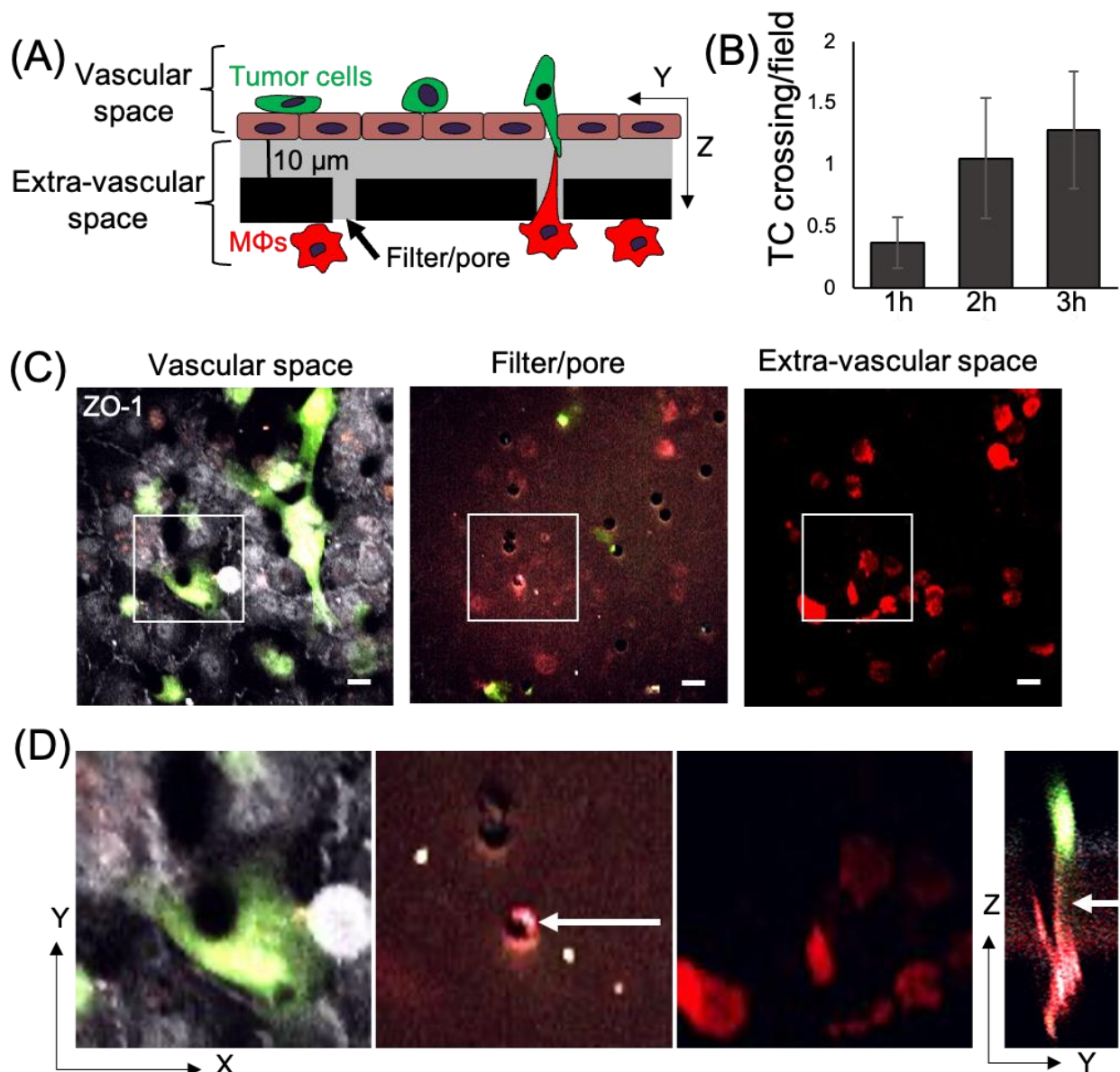


Figure 1. Macrophage TMCs connecting to tumor cells can be detected using an in vitro tumor cell extravasation transendothelial migration (eTEM) assay. (A) Schematic representation of the eTEM assay. The vascular space is contained in the upper part of the chamber and contains green labeled tumor cells on top of a confluent endothelial layer. The endothelial layer is supported by a matrigel (grey) coated filter with 8 μm pores with red labeled macrophages (M Φ s) on the underside of the filter (the extra-vascular space). (B) The number of tumor cells (TC) crossing the endothelium over time was determined as the number per field in the extravascular space. (C) Representative images of the vascular space, the supportive filter, and the extravascular space. Tumor cells and macrophages

are labeled using cell tracker green and cell tracker red, respectively, and endothelial cells are stained for the tight junction marker ZO-1 (white). Note, only tumor cells which cross an intact endothelium (determined by junctional ZO-1 staining in white) are quantified as crossing. If the endothelial monolayer is not intact (lacking junctional ZO-1 staining), tumor cells which may have crossed in this area are excluded from the quantification, shown in figure (B). Scale bar 15 μm (D) Magnified images of the boxed areas in (C) and an orthogonal (Y-Z) view of the Z-stack marked by boxed area in (C). White arrow indicates a TMC formed between a macrophage and tumor cell between the pore of the filter.

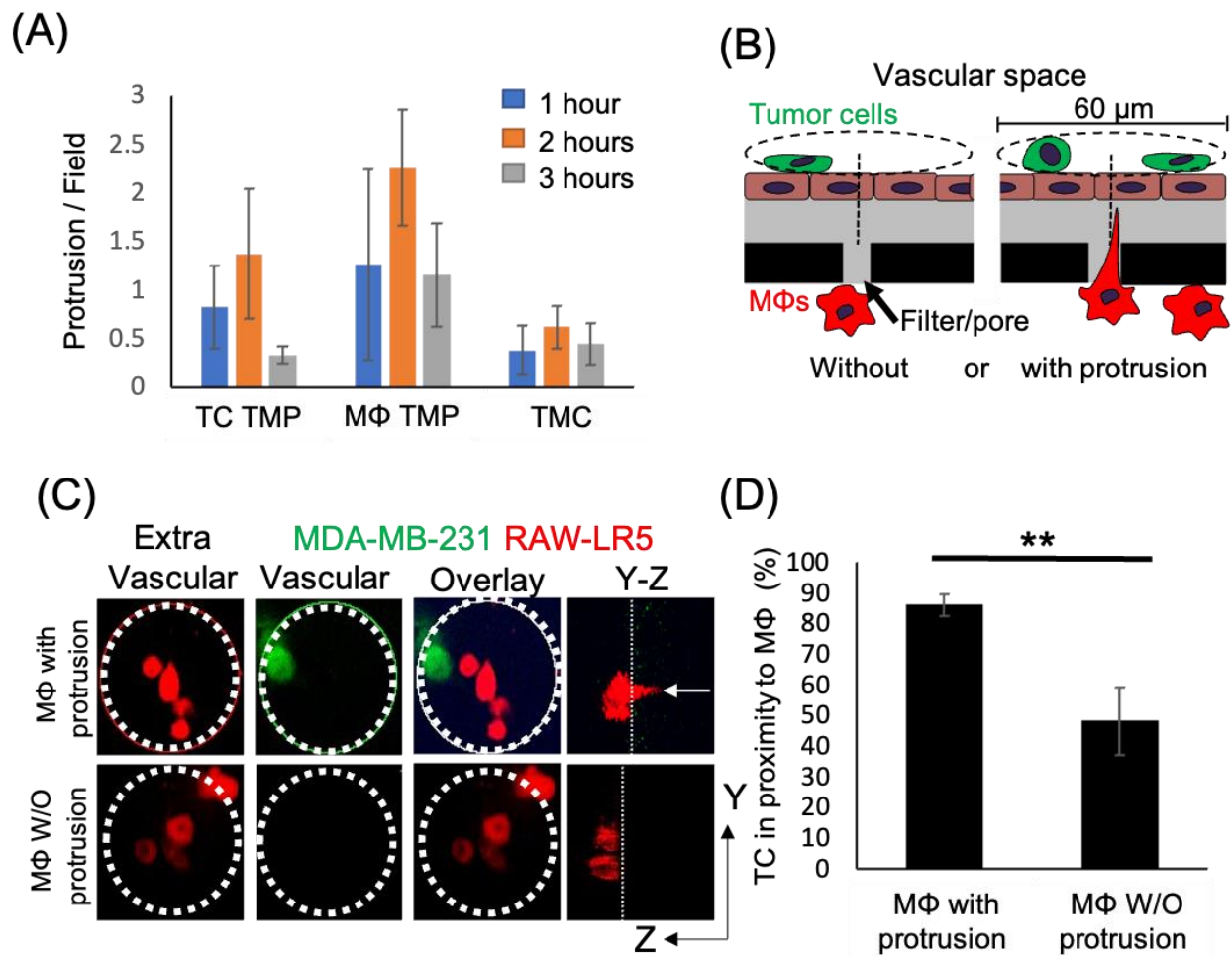


Figure 2. Tumor cell localization to macrophages occurs in high frequency when macrophages contain thin membranous protrusions towards the upper surface. (A) Time course of the formation of thin membranous protrusions (TMP) and thin membranous connections (TMC) over time in the eTEM assay. N = 3 experiments. (B) Schematic of quantification strategy for the proximity assay with green tumor cells located on top of the endothelial layer (brown) in the vascular space and macrophages (red) in the extravascular space. A 60 μm diameter circle (dashed line) is centered around a pore containing macrophages, either with (right) or without (left) protrusions. The presence of tumor cells on the vascular surface within the circle (dashed line) was scored. (C) Representative images of the macrophages (red) in the extravascular space and tumor cells (green) in the vascular space in the eTEM assay 2 h after tumor cell introduction, along with an overlay of the two images to determine the co-localization of both cell types. Dotted white circle represents the analyzed area. White arrow in Y-Z orthogonal view marks the macrophage protrusion crossing the filter. (D) % of the time that tumor cells are found in proximity (within 30 μm radius) to macrophages with and without protrusions. N = 3 experiments, ** p value < 0.01.

The TMCs we detected in the early stage of the extravasation process *in vitro* resembled TNT-like structures that we previously identified to exist between macrophages and tumor cells that were important for tumor cell invasion [33]. Therefore, we hypothesized that the known TNT regulator, M-Sec, would affect the ability of macrophages to promote tumor cell extravasation. To test this hypothesis, we used previously generated macrophage cell lines expressing either a control or an M-Sec targeting shRNA (shCtrl and shM-Sec) [43]. We extended the time of incubation of our *in vitro* eTEM assay to allow for maximal tumor cell crossing into the extravascular space during extravasation (Figure 3A,B). We verified the level of M-Sec in shCtrl and shM-Sec macrophages and the defect in TMC formation. There was a significant 50% reduction in M-Sec protein level in shM-Sec macrophages (Figure S1), which corresponded to a 50% reduction in the capability of these cells to make TMCs (Figure 3C). We then determined the capacity of the shM-Sec macrophages to promote tumor cell extravasation in the eTEM assay, as shown by the analysis of the number of tumor cells crossing the endothelium (Figure 3D). Tumor cells alone have a baseline ability to extravasate that was significantly increased by the presence of shCtrl macrophages. Although shM-Sec macrophages still promoted tumor cell extravasation, this was significantly reduced compared to control macrophages, which was similar to the level of reduction in M-Sec protein levels in these cells. This result shows that macrophage TMCs play an important role in promoting tumor cell extravasation. Next, we determined whether tumor cell extravasation was dependent on soluble factors secreted by macrophages. Macrophage-conditioned media were unable to promote a significant increase in tumor cell extravasation above the baseline level of tumor cells alone (Figure 3D). Overall, these data indicate that macrophages contact tumor cells through TMCs and the reduction in the production of TMCs reduces tumor cell extravasation *in vitro*.

3.2. TMCs Promote Tumor Cell Extravasation *In Vivo*

To verify the importance of macrophage TMCs *in vivo* we generated an M-Sec deficient mouse (M-Sec KO) using CRISPR. We verified the loss of M-Sec by Western blot analysis of isolated bone marrow-derived macrophages (BMMs) from both control and M-Sec KO mice (Figures 4A and S1). We also quantified the ability of the BMMs to produce TMCs *in vitro*, which was reduced almost 60% in the M-Sec KO BMMs (Figure 4B). We also determined whether the reduction in TMC formation in M-Sec KO BMMs in culture was recapitulated in the eTEM assay. As expected, the number of connections between M-Sec KO macrophages and MDA-MB-231 cells was reduced by 70% (Figure 4C). The remaining TMCs in the M-Sec KO BMMs may be due to a residual level of M-Sec being present or because of alternative mechanisms of TMC formation (reviewed in [29,34]). We further investigated if the loss of M-Sec altered the ability of the macrophages to stimulate tumor cell extravasation *in vitro*. In this case, we used a murine metastatic breast tumor cell line expressing GFP (E0771-GFP). In accordance with our hypothesis that macrophage TMCs are critical for the promotion of tumor cell extravasation and our data using the shM-Sec cell line, loss of M-Sec in BMMs also significantly reduced tumor cell extravasation with no significant difference to baseline levels *in vitro* (Figure 4D). This data confirmed that M-Sec KO BMMs recapitulated the data using the shM-Sec cell line (Figure 3D) and suggested that the M-Sec KO mouse model can provide valuable *in vivo* data.

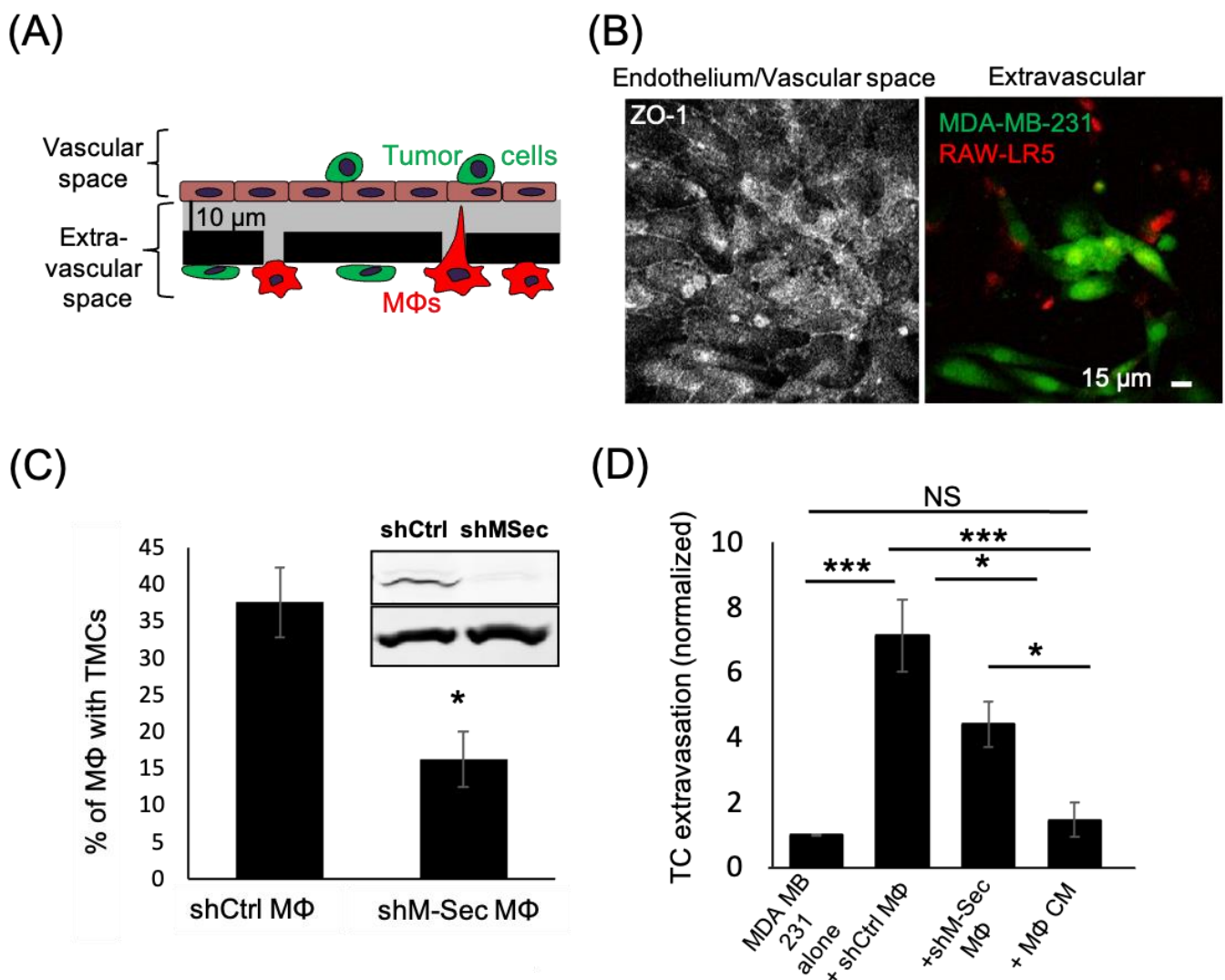


Figure 3. Macrophages defective in TMCs do not promote tumor cell extravasation. **(A)** Schematic representation of eTEM assay after overnight incubation to allow for maximal tumor cell crossing. The vascular space is contained in the upper part of the chamber and contains green labeled tumor cells on top of a confluent endothelial layer. The endothelial layer is supported by a matrigel (grey) coated filter with 8 µm pores with red labeled macrophages (MΦs) on the underside of the filter (the extravascular space). **(B)** Representative images of the intact endothelium stained for ZO-1 (left) in the vascular space and (right) the tumor cells (green) that have crossed into the extravascular space 24 h after tumor cell addition. **(C)** shRNA Control (shCtrl MΦ) or shRNA M-Sec (shM-Sec MΦ) macrophages were cultured overnight and the percentage of macrophages making TMCs between cells quantified. Inset-Western Blot showing M-Sec protein (upper) and actin (lower) level in macrophages expressing either shRNA control (shCtrl) or shRNA M-Sec (shM-Sec). Uncropped blot is shown in Figure S1. **(D)** The number of MDA-MB-231 tumor cells (TC) crossing the endothelial layer into the extravascular space after 24 h in absence (alone) or presence of RAW/LR5 macrophages that express shRNA Control (shCtrl MΦ) or shRNA M-Sec (shM-Sec MΦ), or in the presence of MΦ conditioned media (CM). The number of TCs present in the extravascular space, normalized to the number of TCs crossing alone. 25 fields per condition were analyzed for each of 3 independent experiments. * $p < 0.05$, *** $p < 0.001$, NS = non-significant.

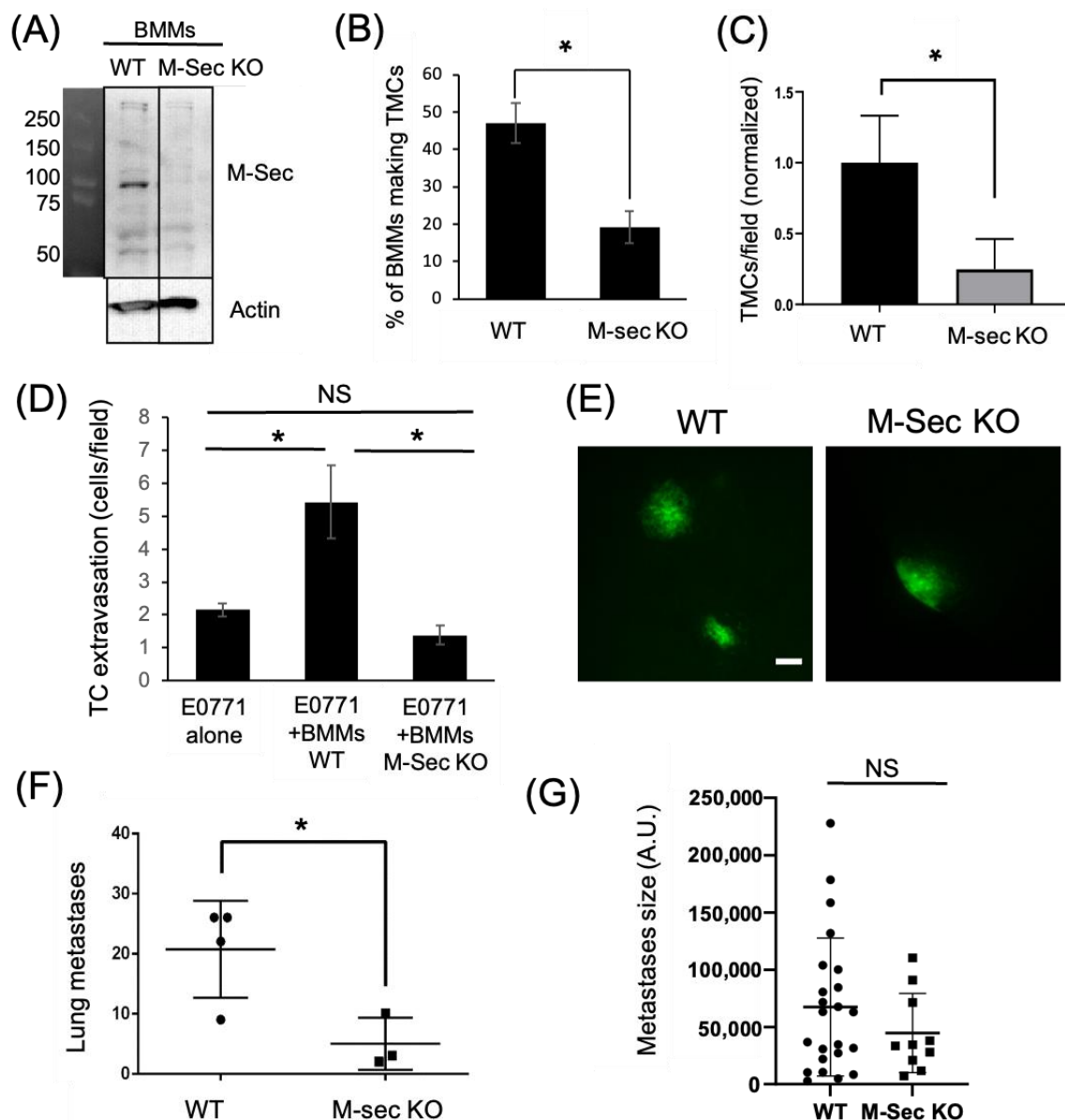


Figure 4. Tumor cell extravasation is impaired in vitro and in vivo by macrophages lacking the ability to form TMCs. **(A)** Western Blot showing M-Sec level in bone marrow derived macrophages (BMMs) isolated from either WT or M-Sec KO mice. Uncropped blot is shown in Figure S1. **(B)** WT or M-Sec KO BMMs were cultured overnight on a 35 mm MatTek™ dish and the percentage of BMMs making TMCs between macrophages and tumor cells determined. The results show a decreased ability of M-Sec KO BMMs to produce TMCs in vitro. **(C)** Quantification of TMCs formed between MDA-MB-231 cells and either WT or M-Sec KO BMMs across the endothelium 2 h after tumor cell introduction to the eTEM assay (N = 3 experiments) shows a reduction in the TMCs formed in vitro in the eTEM assay. **(D)** Quantification of GFP-E0771 tumor cells (TC) crossing the endothelium in the absence or presence of wild type (BMMs WT) or M-Sec deficient (BMMs KO M-Sec) in the eTEM assay. N = 3 experiments, 36 fields per experiment for each condition where analyzed. The results show that BMMs defective in forming TMCs impacted tumor cells extravasation. **(E)** Representative images of lung metastases derived from GFP-E0771 cells injected in the tail vein of either WT or M-Sec KO mice 7 days after tumor cell injection, scale-bar 100 μ m. Widefield images can be found in Figure S2. **(F)** Quantification of total number of metastases in either WT or M-Sec KO mice injected with E0771-GFP. (N = 4 for WT and N = 3 for M-Sec KO). **(G)** Quantification of metastasis size, per field. (N = 4 for WT and N = 3 for M-Sec KO). For all—* $p < 0.05$, NS = non-significant.

To determine if macrophage M-Sec dependent TMC formation was important for tumor cell extravasation *in vivo*, we injected syngeneic E0771-GFP into the tail vein of either WT or M-Sec KO mice. One week post injection, the animals were sacrificed and the lungs analyzed for metastatic burden. The lungs of all mice contained tumor cells on the surface (Figure 4E). Following quantification of metastatic lesions, it was revealed that the M-Sec KO animals had a significantly lower number of metastases compared to the WT animals (Figure 4F). The reduction in metastases was not due to cell growth as there was no significant difference in the size of the individual metastases (Figure 4G).

Previous studies showed that macrophages extend extremely long, thin pseudopods when in proximity to tumor cells [21], but protrusions across the endothelium had not been previously identified. To determine if TMCs occurred during tumor cell extravasation *in vivo*, we utilized the WHRIL (window for high-resolution imaging of the lung) with an experimental metastasis model to obtain high-resolution images of tumor cell extravasation into the lungs [22]. E0771-GFP cells were injected into the tail vein of mice expressing td tomato under the VE-Cadherin promoter to label the vasculature and ECFP under the control of the CSF1r promoter in order to label the macrophages. Images of the tumor cells in the blood vessels of the lungs were collected in 3D over time following injection. When tumor cells reach the lungs, they become lodged and can spend hours trapped in the capillary beds in the lungs before they ultimately extravasate, die, or become dislodged [13]. We examined z-slices with stationary tumor cells in the blood vessels for the presence of macrophages in the lung parenchyma that extend protrusions through the intact blood vessel endothelium to reach the tumor cell in the blood vessel, creating a TMC (Figure 5). We observed an interaction between a stationary tumor cell in the vascular space and a macrophage in the extravascular space, mediated by a long thin tube which crossed through the endothelium (seen in Figure 5A), and that this interaction preceded tumor cell extravasation into the lung parenchyma (Figure 5D). This suggests that macrophages contact tumor cells through TMCs, which may initiate or enhance tumor cell crossing.

Taken together, these data support the importance of TMCs in the metastatic process and, in particular, highlight the possible role of TMCs in promoting the extravasation of disseminated tumor cells.

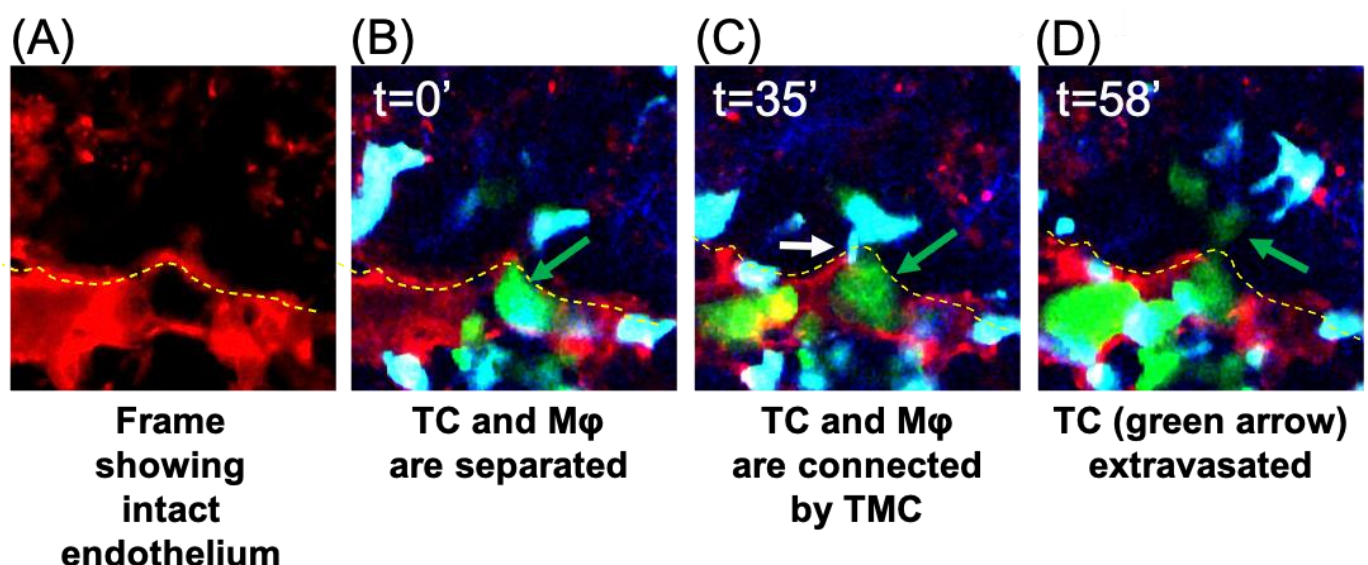


Figure 5. IVI of tumor cell extravasation to the lung reveals the presence of a thin membranous connection (TMC) from a tissue macrophage contacting a circulating tumor cell prior to tumor cell extravasation. Tumor cells were injected through the tail vein in mice bearing a WHRIL (window for high-resolution imaging of the lung) which was surgically implanted over the lungs of mice expressing ECFP in macrophages and td-tomato labeled vasculature. Within a few minutes post injection of tumor cells, images were collected over time. (A) Representative image showing the intact

endothelium (red) of the lung capillary. **(B)** Representative image of a stationary E0771-GFP tumor cell (green) in a lung capillary at the point at which it is arrested in the vasculature ($t = 0'$). This tumor cell was followed throughout the extravasation process and is indicated by the green arrow in each panel. **(C)** A TMC (white arrow) protruding from the macrophage and connecting to the stationary intravascular tumor cell in panel B indicated by the green arrow ($t = 35'$). **(D)** Tumor cell indicated in panels B and C has extravasated into the lung parenchyma (green arrow). In all images, a yellow dashed line indicates the intact blood vessel endothelium (red) of the lung capillary (seen in **(A)**) separating circulating tumor cells (green) and macrophages (blue) that reside the parenchyma.

4. Discussion

Metastasis is estimated to be responsible for approximately two thirds of cancer-related mortality [44]. The importance of macrophages in promoting metastatic dissemination and growth in primary as well as secondary breast cancers is well known [3,5,6]. In this work, we focused our attention on the role of macrophages in tumor cell extravasation and, in particular, on the physical interaction between macrophages and tumor cells that reside on opposing sides of the lung vasculature. We were able to identify TMCs in an *in vitro* assay that mimics the extravasation process. Similar barrier-crossing membranous extensions have already been described to be made by different immune cells *in vivo*. Dendritic cells send dendrites outside the epithelium to sample bacteria in the intestinal lumen [45] and hematopoietic stem cells send TMCs across the dense basement membranes to deliver lysosomes into diseased proximal tubular cells when grafted to cystinotic kidneys [46]. However, we are the first to show a connection between tumor cells and macrophages in the context of the metastases both *in vitro* and their importance in tumor cell extravasation *in vivo*.

Our previous work has shown that similar structures that we identified as TNTs, a subset of TMCs, were important in promoting tumor cell invasion and dissemination [33]. We confirmed that the TMCs that we detected during extravasation were regulated in the same manner as TNTs by using macrophages with reduced levels of M-Sec, a known regulator of the TNTs [33,36,40,47]. The reduction in M-Sec decreased TMC formation between macrophages and tumor cells and reduced tumor cells extravasation *in vitro*. Taken together, these data suggest that physical contact between tumor cells and macrophages promote tumor cell extravasation through TMCs. To further investigate the role of macrophage TMCs in metastatic seeding, we generated a mouse model for M-Sec deficiency by introducing a single-point mutation in the M-Sec gene through CRISPR technology. BMMs isolated from the M-Sec KO mouse presented a lower capability of making TMCs and were not able to promote extravasation of tumor cells *in vitro*. These results give us confidence that macrophages generated from M-Sec KO mouse recapitulates our results using macrophage cell lines.

Our initial intravital imaging of macrophages interacting with tumor cells during extravasation *in vivo* suggests that macrophages contact tumor cells through TMCs, which may initiate or enhance trans-endothelial migration of tumor cells. Additional studies are needed in order to determine the frequency and kinetics of macrophage TMC contact with tumor cells *in vivo* before, during, and after extravasation.

The importance of M-Sec and TNTs/TMCs *in vivo* was recently demonstrated by another group that showed that M-Sec-TNTs played a protective role in the glomeruli by rescuing podocytes via mitochondrial horizontal transfer [40]. We tested the capability of injected wild type tumor cells to disseminate into the lung parenchyma of M-Sec KO mice. The number of metastases in the M-Sec KO mice was significantly reduced compared to wild type mice, indicating a role for M-Sec in regulating metastatic dissemination in the lung microenvironment. Taking into consideration that there was no significant change in the size of the metastases, we believe that M-Sec generation of TMCs is important for the seeding of circulating tumor cells into the lung parenchyma and not for the growth of seeded tumor cells. Others have shown that factors such as Flt-1 regulate the growth [48].

While we showed direct macrophage contact facilitated tumor cell extravasation, which could not be accomplished via secreted factors in conditioned media *in vitro*, this does not mean that there is not a role for secreted factors in the process. For example, MAMs which originate from circulating inflammatory monocytes are recruited by the CC-chemokine ligand 2 (CCL2) and, once recruited, MAMs secrete another chemokine, CCL3, which leads to MAM retention [19]. A number of genes are upregulated in MAMs compared to resident lung or splenic macrophages that may regulate the ability to generate TMCs in macrophages. Ongoing studies are focused on determining the factors regulating macrophage TMCs MAMs. Additionally, tumor cell-derived factors may account for the association of macrophage protrusions with tumor cells opposite to the endothelium, but defining which chemokine is contributing to this process is a topic for future study.

Finally, most mechanistic *in vitro* studies on TMC have been conducted using two-dimensional (2D) culture systems, with TMC being formed above the substrate in a three-dimensional (3D) space. We have detected the presence of tumor cell TMCs in 3D matrices of collagen [47] and others have detected TMCs in 3D bioprinted scaffolds [49]. Additionally, several studies have demonstrated the effects of different extracellular matrix (ECM) materials on TMC formation in 3D [50,51]. While we have not explored the role of the extracellular matrix in this particular study, we have employed an *in vitro* eTEM assay containing ECM that mimics the *in vivo* 3D environment present in the metastatic niche during tumor cell extravasation. Even though many aspects of TMCs (such as the molecular mechanisms that drive them or how they promote tumor cells extravasation) are still unknown, our data point towards an important role of TMCs in promoting tumor cell extravasation at the secondary site.

5. Conclusions

In summary, we have found that thin membranous connections (TMCs) form between macrophages and tumor cells, and these connections stimulate tumor cell extravasation. We found that TMC-driven tumor cell extravasation required the expression of M-Sec, a TNT regulator, in macrophages. Additionally, breast cancer metastatic burden to the lungs was reduced in M-Sec knockout mice. These findings indicate that macrophage TMCs are critical for tumor cell extravasation and underscore the therapeutic potential of targeting TMCs to reduce metastasis.

Supplementary Materials: The following supporting information can be downloaded at: <https://www.mdpi.com/article/10.3390/cancers15072092/s1>, Figure S1: Detection of M-Sec protein levels in the various macrophages used in this study; Figure S2: Widefield images of GFP-E0771 lung metastases in WT and M-Sec KO mice.

Author Contributions: Conceptualization, D.C. and J.S.C.; methodology, A.G.; software, A.G.; validation, A.G., D.C. and C.L.D.; formal analysis, A.G. and D.C.; investigation, A.G.; resources, D.C., D.E. and J.S.C.; data curation, A.G., C.L.D. and D.E.; writing—original draft preparation, A.G. and D.C.; writing—review and editing, A.G., D.C. and C.L.D.; visualization, A.G., D.C., C.L.D. and J.S.C.; supervision, D.C. and J.S.C.; project administration, D.C.; funding acquisition, D.C., D.E. and J.S.C. All authors have read and agreed to the published version of the manuscript.

Funding: This work was supported by the NCI grants F32-CA243350 (CLD), R01 CA216248 (JSC & DE) and P01 CA257885 (JSC & DE), The Gruss-Lipper Biophotonics Center, The Integrated Imaging Program, the Integrated Imaging Program for Cancer Research, The Evelyn Gruss-Lipper Charitable Foundation, and The Helen & Irving Spatz Foundation. CLD was partially funded under a K12 GM102779 (DC) IRACDA fellowship where the content is solely the responsibility of the authors and does not necessarily represent the official views of the K12 support.

Institutional Review Board Statement: All procedures were conducted in accordance with the National Institutes of Health regulation concerning the care and use of experimental animals and with the approval of Albert Einstein College of Medicine Animal Care and Use Committee (protocol 00001274) in keeping with OLAW Assurance and AAALAC accreditation.

Informed Consent Statement: Not applicable.

Data Availability Statement: All data generated in the study is contained within the article and Supplementary Material.

Acknowledgments: The authors would like to thank Lalage Wakefield’s lab at the NCI for the donation of the E0771 cell line. The authors would like to thank the Montefiore Einstein Cancer Center, the Analytical Imaging Facility, and the Gene Modification and Transgenic Mouse Facility of Albert Einstein College of Medicine. This work was supported by the NCI grants F32-CA243350 (CLD), R01 CA216248 (JSC & DE) and P01 CA257885 (JSC & DE), The Gruss-Lipper Biophotonics Center, The Integrated Imaging Program, the Integrated Imaging Program for Cancer Research, and The Evelyn Gruss-Lipper Charitable Foundation. CLD was partially funded under a K12 GM102779 (DC) IRACDA fellowship where the content is solely the responsibility of the authors and does not necessarily represent the official views of the K12 support.

Conflicts of Interest: The authors declare no conflict of interest.

References

1. Siegel, R.L.; Miller, K.D.; Fuchs, H.E.; Jemal, A. Cancer Statistics, 2021. *CA Cancer J. Clin.* **2021**, *71*, 7–33. [\[CrossRef\]](#)
2. Wyckoff, J.; Wang, W.; Lin, E.Y.; Wang, Y.; Pixley, F.; Stanley, E.R.; Graf, T.; Pollard, J.W.; Segall, J.; Condeelis, J. A paracrine loop between tumor cells and macrophages is required for tumor cell migration in mammary tumors. *Cancer Res.* **2004**, *64*, 7022–7029. [\[CrossRef\]](#) [\[PubMed\]](#)
3. Condeelis, J.; Pollard, J.W. Macrophages: Obligate partners for tumor cell migration, invasion, and metastasis. *Cell* **2006**, *124*, 263–266. [\[CrossRef\]](#) [\[PubMed\]](#)
4. Karagiannis, G.S.; Condeelis, J.S.; Oktay, M.H. Chemotherapy-Induced Metastasis: Molecular Mechanisms, Clinical Manifestations, Therapeutic Interventions. *Cancer Res.* **2019**, *79*, 4567–4576. [\[CrossRef\]](#) [\[PubMed\]](#)
5. Sharma, V.P.; Tang, B.; Wang, Y.; Duran, C.L.; Karagiannis, G.S.; Xue, E.A.; Entenberg, D.; Borriello, L.; Coste, A.; Eddy, R.J.; et al. Live tumor imaging shows macrophage induction and TMEM-mediated enrichment of cancer stem cells during metastatic dissemination. *Nat. Commun.* **2021**, *12*, 7300. [\[CrossRef\]](#)
6. Borriello, L.; Karagiannis, G.S.; Duran, C.L.; Coste, A.; Oktay, M.H.; Entenberg, D.; Condeelis, J.S. The role of the tumor microenvironment in tumor cell intravasation and dissemination. *Eur. J. Cell Biol.* **2020**, *99*, 151098. [\[CrossRef\]](#)
7. Bingle, L.; Brown, N.J.; Lewis, C.E. The role of tumour-associated macrophages in tumour progression: Implications for new anticancer therapies. *J. Pathol.* **2002**, *196*, 254–265. [\[CrossRef\]](#)
8. Karagiannis, G.S.; Pastoriza, J.M.; Wang, Y.; Harney, A.S.; Entenberg, D.; Pignatelli, J.; Sharma, V.P.; Xue, E.A.; Cheng, E.; D’Alfonso, T.M.; et al. Neoadjuvant chemotherapy induces breast cancer metastasis through a TMEM-mediated mechanism. *Sci. Transl. Med.* **2017**, *9*, eaan0026. [\[CrossRef\]](#)
9. Goswami, S.; Sahai, E.; Wyckoff, J.B.; Cammer, M.; Cox, D.; Pixley, F.J.; Stanley, E.R.; Segall, J.E.; Condeelis, J.S. Macrophages promote the invasion of breast carcinoma cells via a colony-stimulating factor-1/epidermal growth factor paracrine loop. *Cancer Res.* **2005**, *65*, 5278–5283. [\[CrossRef\]](#)
10. Roussos, E.T.; Balsamo, M.; Alford, S.K.; Wyckoff, J.B.; Gligorijevic, B.; Wang, Y.; Pozzuto, M.; Stobezki, R.; Goswami, S.; Segall, J.E.; et al. Mena invasive (MenaINV) promotes multicellular streaming motility and transendothelial migration in a mouse model of breast cancer. *J. Cell Sci.* **2011**, *124*, 2120–2131. [\[CrossRef\]](#)
11. Leung, E.; Xue, A.; Wang, Y.; Rougerie, P.; Sharma, V.P.; Eddy, R.; Cox, D.; Condeelis, J. Blood vessel endothelium-directed tumor cell streaming in breast tumors requires the HGF/C-Met signaling pathway. *Oncogene* **2017**, *36*, 2680–2692. [\[CrossRef\]](#)
12. Harney, A.S.; Arwert, E.N.; Entenberg, D.; Wang, Y.; Guo, P.; Qian, B.Z.; Oktay, M.H.; Pollard, J.W.; Jones, J.G.; Condeelis, J.S. Real-Time Imaging Reveals Local, Transient Vascular Permeability, and Tumor Cell Intravasation Stimulated by TIE2hi Macrophage-Derived VEGFA. *Cancer Discov.* **2015**, *5*, 932–943. [\[CrossRef\]](#) [\[PubMed\]](#)
13. Borriello, L.; Coste, A.; Traub, B.; Sharma, V.P.; Karagiannis, G.S.; Lin, Y.; Wang, Y.; Ye, X.; Duran, C.L.; Chen, X.; et al. Primary tumor associated macrophages activate programs of invasion and dormancy in disseminating tumor cells. *Nat. Commun.* **2022**, *13*, 626. [\[CrossRef\]](#)
14. Lin, E.Y.; Nguyen, A.V.; Russell, R.G.; Pollard, J.W. Colony-stimulating factor 1 promotes progression of mammary tumors to malignancy. *J. Exp. Med.* **2001**, *193*, 727–740. [\[CrossRef\]](#) [\[PubMed\]](#)
15. Lin, E.Y.; Jones, J.G.; Li, P.; Zhu, L.; Whitney, K.D.; Muller, W.J.; Pollard, J.W. Progression to malignancy in the polyoma middle T oncoprotein mouse breast cancer model provides a reliable model for human diseases. *Am. J. Pathol.* **2003**, *163*, 2113–2126. [\[CrossRef\]](#)
16. Qian, B.Z.; Li, J.; Zhang, H.; Kitamura, T.; Zhang, J.; Campion, L.R.; Kaiser, E.A.; Snyder, L.A.; Pollard, J.W. CCL2 recruits inflammatory monocytes to facilitate breast-tumour metastasis. *Nature* **2011**, *475*, 222–225. [\[CrossRef\]](#)
17. Qian, B.Z.; Pollard, J.W. New tricks for metastasis-associated macrophages. *Breast Cancer Res.* **2012**, *14*, 316. [\[CrossRef\]](#)
18. Qian, B.; Deng, Y.; Im, J.H.; Muschel, R.J.; Zou, Y.; Li, J.; Lang, R.A.; Pollard, J.W. A distinct macrophage population mediates metastatic breast cancer cell extravasation, establishment and growth. *PLoS ONE* **2009**, *4*, e6562. [\[CrossRef\]](#)

19. Kitamura, T.; Qian, B.Z.; Soong, D.; Cassetta, L.; Noy, R.; Sugano, G.; Kato, Y.; Li, J.; Pollard, J.W. CCL2-induced chemokine cascade promotes breast cancer metastasis by enhancing retention of metastasis-associated macrophages. *J. Exp. Med.* **2015**, *212*, 1043–1059. [\[CrossRef\]](#)
20. Rodriguez-Tirado, C.; Entenberg, D.; Li, J.; Qian, B.Z.; Condeelis, J.S.; Pollard, J.W. Interleukin 4 Controls the Pro-Tumoral Role of Macrophages in Mammary Cancer Pulmonary Metastasis in Mice. *Cancers* **2022**, *14*, 4336. [\[CrossRef\]](#) [\[PubMed\]](#)
21. Entenberg, D.; Rodriguez-Tirado, C.; Kato, Y.; Kitamura, T.; Pollard, J.W.; Condeelis, J. In vivo subcellular resolution optical imaging in the lung reveals early metastatic proliferation and motility. *Intravital* **2015**, *4*, 1–11. [\[CrossRef\]](#) [\[PubMed\]](#)
22. Entenberg, D.; Voiculescu, S.; Guo, P.; Borriello, L.; Wang, Y.; Karagiannis, G.S.; Jones, J.; Baccay, F.; Oktay, M.; Condeelis, J. A permanent window for the murine lung enables high-resolution imaging of cancer metastasis. *Nat. Methods* **2018**, *15*, 73–80. [\[CrossRef\]](#)
23. Chinnery, H.R.; Pearlman, E.; McMenamin, P.G. Cutting edge: Membrane nanotubes in vivo: A feature of MHC class II+ cells in the mouse cornea. *J. Immunol.* **2008**, *180*, 5779–5783. [\[CrossRef\]](#) [\[PubMed\]](#)
24. Rehberg, M.; Nekolla, K.; Sellner, S.; Praetner, M.; Mildner, K.; Zeuschner, D.; Krombach, F. Intercellular Transport of Nanomaterials is Mediated by Membrane Nanotubes In Vivo. *Small* **2016**, *12*, 1882–1890. [\[CrossRef\]](#) [\[PubMed\]](#)
25. Alarcon-Martinez, L.; Villafranca-Baughman, D.; Quintero, H.; Kacerovsky, J.B.; Dotigny, F.; Murai, K.K.; Prat, A.; Drapeau, P.; Di Polo, A. Interpericyte tunnelling nanotubes regulate neurovascular coupling. *Nature* **2020**, *585*, 91–95. [\[CrossRef\]](#)
26. Lou, E.; Fujisawa, S.; Barlas, A.; Romin, Y.; Manova-Todorova, K.; Moore, M.A.; Subramanian, S. Tunneling Nanotubes: A new paradigm for studying intercellular communication and therapeutics in cancer. *Commun. Integr. Biol.* **2012**, *5*, 399–403. [\[CrossRef\]](#) [\[PubMed\]](#)
27. Osswald, M.; Jung, E.; Sahm, F.; Solecki, G.; Venkataramani, V.; Blaes, J.; Weil, S.; Horstmann, H.; Wiestler, B.; Syed, M.; et al. Brain tumour cells interconnect to a functional and resistant network. *Nature* **2015**, *528*, 93–98. [\[CrossRef\]](#) [\[PubMed\]](#)
28. Weil, S.; Osswald, M.; Solecki, G.; Grosch, J.; Jung, E.; Lemke, D.; Ratliff, M.; Hanggi, D.; Wick, W.; Winkler, F. Tumor microtubes convey resistance to surgical lesions and chemotherapy in gliomas. *Neuro Oncol.* **2017**, *19*, 1316–1326. [\[CrossRef\]](#) [\[PubMed\]](#)
29. Abounit, S.; Zurzolo, C. Wiring through tunneling nanotubes—from electrical signals to organelle transfer. *J. Cell Sci.* **2012**, *125*, 1089–1098. [\[CrossRef\]](#)
30. Lou, E.; Fujisawa, S.; Morozov, A.; Barlas, A.; Romin, Y.; Dogan, Y.; Gholami, S.; Moreira, A.L.; Manova-Todorova, K.; Moore, M.A. Tunneling nanotubes provide a unique conduit for intercellular transfer of cellular contents in human malignant pleural mesothelioma. *PLoS ONE* **2012**, *7*, e33093. [\[CrossRef\]](#)
31. Jackson, M.V.; Morrison, T.J.; Doherty, D.F.; McAuley, D.F.; Matthay, M.A.; Kissenpfennig, A.; O’Kane, C.M.; Krasnodembskaya, A.D. Mitochondrial Transfer via Tunneling Nanotubes is an Important Mechanism by Which Mesenchymal Stem Cells Enhance Macrophage Phagocytosis in the In Vitro and In Vivo Models of ARDS. *Stem Cells* **2016**, *34*, 2210–2223. [\[CrossRef\]](#) [\[PubMed\]](#)
32. Burt, R.; Dey, A.; Aref, S.; Aguiar, M.; Akarca, A.; Bailey, K.; Day, W.; Hooper, S.; Kirkwood, A.; Kirschner, K.; et al. Activated stromal cells transfer mitochondria to rescue acute lymphoblastic leukemia cells from oxidative stress. *Blood* **2019**, *134*, 1415–1429. [\[CrossRef\]](#) [\[PubMed\]](#)
33. Hanna, S.J.; McCoy-Simandle, K.; Leung, E.; Genna, A.; Condeelis, J.; Cox, D. Tunneling nanotubes, a novel mode of tumor cell-macrophage communication in tumor cell invasion. *J. Cell Sci.* **2019**, *132*, jcs223321. [\[CrossRef\]](#) [\[PubMed\]](#)
34. McCoy-Simandle, K.; Hanna, S.J.; Cox, D. Exosomes and nanotubes: Control of immune cell communication. *Int. J. Biochem. Cell Biol.* **2016**, *71*, 44–54. [\[CrossRef\]](#)
35. Roehlecke, C.; Schmidt, M.H.H. Tunneling Nanotubes and Tumor Microtubes in Cancer. *Cancers* **2020**, *12*, 857. [\[CrossRef\]](#) [\[PubMed\]](#)
36. Hase, K.; Kimura, S.; Takatsu, H.; Ohmae, M.; Kawano, S.; Kitamura, H.; Ito, M.; Watarai, H.; Hazelett, C.C.; Yeaman, C.; et al. M-Sec promotes membrane nanotube formation by interacting with Ral and the exocyst complex. *Nat. Cell Biol.* **2009**, *11*, 1427–1432. [\[CrossRef\]](#)
37. Kimura, S.; Yamashita, M.; Yamakami-Kimura, M.; Sato, Y.; Yamagata, A.; Kobashigawa, Y.; Inagaki, F.; Amada, T.; Hase, K.; Iwanaga, T.; et al. Distinct Roles for the N- and C-terminal Regions of M-Sec in Plasma Membrane Deformation during Tunneling Nanotube Formation. *Sci. Rep.* **2016**, *6*, 33548. [\[CrossRef\]](#)
38. Cox, D.; Chang, P.; Zhang, Q.; Reddy, P.G.; Bokoch, G.M.; Greenberg, S. Requirements for both Rac1 and Cdc42 in membrane ruffling and phagocytosis in leukocytes. *J. Exp. Med.* **1997**, *186*, 1487–1494. [\[CrossRef\]](#)
39. Stanley, E.R. Murine bone marrow-derived macrophages. *Methods Mol. Biol.* **1997**, *75*, 301–304. [\[CrossRef\]](#)
40. Barutta, F.; Kimura, S.; Hase, K.; Bellini, S.; Corbetta, B.; Corbelli, A.; Fiordaliso, F.; Barreca, A.; Papotti, M.G.; Ghiggeri, G.M.; et al. Protective Role of the M-Sec-Tunneling Nanotube System in Podocytes. *J. Am. Soc. Nephrol.* **2021**, *32*, 1114–1130. [\[CrossRef\]](#)
41. Entenberg, D.; Wyckoff, J.; Gligorijevic, B.; Roussos, E.T.; Verkhusha, V.V.; Pollard, J.W.; Condeelis, J. Setup and use of a two-laser multiphoton microscope for multichannel intravital fluorescence imaging. *Nat. Protoc.* **2011**, *6*, 1500–1520. [\[CrossRef\]](#)
42. Borriello, L.; Traub, B.; Coste, A.; Oktay, M.H.; Entenberg, D. A Permanent Window for Investigating Cancer Metastasis to the Lung. *J. Vis. Exp.* **2021**, *173*, e62761. [\[CrossRef\]](#)
43. Hanna, S.J.; McCoy-Simandle, K.; Miskolci, V.; Guo, P.; Cammer, M.; Hodgson, L.; Cox, D. The Role of Rho-GTPases and actin polymerization during Macrophage Tunneling Nanotube Biogenesis. *Sci. Rep.* **2017**, *7*, 8547. [\[CrossRef\]](#) [\[PubMed\]](#)
44. Dillekas, H.; Rogers, M.S.; Straume, O. Are 90% of deaths from cancer caused by metastases? *Cancer Med.* **2019**, *8*, 5574–5576. [\[CrossRef\]](#) [\[PubMed\]](#)

45. Rescigno, M.; Rotta, G.; Valzasina, B.; Ricciardi-Castagnoli, P. Dendritic cells shuttle microbes across gut epithelial monolayers. *Immunobiology* **2001**, *204*, 572–581. [[CrossRef](#)]
46. Naphade, S.; Sharma, J.; Gaide Chevronnay, H.P.; Shook, M.A.; Yeagy, B.A.; Rocca, C.J.; Ur, S.N.; Lau, A.J.; Courtoy, P.J.; Cherqui, S. Brief reports: Lysosomal cross-correction by hematopoietic stem cell-derived macrophages via tunneling nanotubes. *Stem Cells* **2015**, *33*, 301–309. [[CrossRef](#)]
47. Carter, K.P.; Hanna, S.; Genna, A.; Lewis, D.; Segall, J.E.; Cox, D. Macrophages enhance 3D invasion in a breast cancer cell line by induction of tumor cell tunneling nanotubes. *Cancer Rep.* **2019**, *2*, e1213. [[CrossRef](#)]
48. Qian, B.Z.; Zhang, H.; Li, J.; He, T.; Yeo, E.J.; Soong, D.Y.; Carragher, N.O.; Munro, A.; Chang, A.; Bresnick, A.R.; et al. FLT1 signaling in metastasis-associated macrophages activates an inflammatory signature that promotes breast cancer metastasis. *J. Exp. Med.* **2015**, *212*, 1433–1448. [[CrossRef](#)]
49. Herrada-Manchon, H.; Celada, L.; Rodriguez-Gonzalez, D.; Alejandro Fernandez, M.; Aguilar, E.; Chiara, M.D. Three-dimensional bioprinted cancer models: A powerful platform for investigating tunneling nanotube-like cell structures in complex microenvironments. *Mater. Sci. Eng. C Mater. Biol. Appl.* **2021**, *128*, 112357. [[CrossRef](#)]
50. Franchi, M.; Piperigkou, Z.; Riti, E.; Masola, V.; Onisto, M.; Karamanos, N.K. Long filopodia and tunneling nanotubes define new phenotypes of breast cancer cells in 3D cultures. *Matrix Biol. Plus* **2020**, *6–7*, 100026. [[CrossRef](#)]
51. Jana, A.; Ladner, K.; Lou, E.; Nain, A.S. Tunneling Nanotubes between Cells Migrating in ECM Mimicking Fibrous Environments. *Cancers* **2022**, *14*, 1989. [[CrossRef](#)] [[PubMed](#)]

Disclaimer/Publisher’s Note: The statements, opinions and data contained in all publications are solely those of the individual author(s) and contributor(s) and not of MDPI and/or the editor(s). MDPI and/or the editor(s) disclaim responsibility for any injury to people or property resulting from any ideas, methods, instructions or products referred to in the content.